buildings

MDPI

Article

Impact of Fibres on the Mechanical and Durable Behaviour of Fibre-Reinforced Concrete

Florence More Dattu Shanker More and Senthil Selvan Subramanian *

Department of Civil Engineering, SRMIST, Maraimalai Nagar, Kattankulathur 603203, India
* Correspondence: senthils10@srmist.edu.in

Abstract: Numerous studies have been conducted recently on fibre reinforced concrete (FRC), a material that is frequently utilized in the building sector. The utilization of FRC has grown in relevance recently due to its enhanced mechanical qualities over normal concrete. Due to increased environmental degradation in recent years, natural fibres were developed and research is underway with the goal of implementing them in the construction industry. In this work, several natural and artificial fibres, including glass, carbon, steel, jute, coir, and sisal fibres are used to experimentally investigate the mechanical and durability properties of fibre-reinforced concrete. The fibres were added to the M40 concrete mix with a volumetric ratio of 0%, 0.5%, 1.0%, 1.5%, 2.0% and 2.5%. The compressive strength of the conventional concrete and fibre reinforced concrete with the addition of 1.5% steel, 1.5% carbon, 1.0% glass, 2.0% coir, 1.5% jute and 1.5% sisal fibres were 4.2 N/mm^2, 45.7 N/mm^2, 41.5 N/mm^2, 45.7 N/mm^2, 46.6 N/mm^2, 45.7 N/mm^2 and 45.9 N/mm^2, respectively. Comparing steel fibre reinforced concrete to regular concrete results in a 13.69% improvement in compressive strength. Similarly, the compressive strengths were increased by 3.24%, 13.69%, 15.92%, 13.68% and 14.18% for carbon, glass, coir, jute, and sisal fibre reinforced concrete respectively when equated with plain concrete. With the optimum fraction of fibre reinforced concrete, mechanical and durability qualities were experimentally investigated. A variety of durability conditions, including the Rapid Chloride Permeability Test, water absorption, porosity, sorptivity, acid attack, alkali attack, and sulphate attack, were used to study the behaviour of fiber reinforced concrete. When compared to conventional concrete, natural fibre reinforced concrete was found to have higher water absorption and sorptivity. The rate of acid and chloride attacks on concrete reinforced with natural fibres was significantly high. The artificial fibre reinforced concrete was found to be more efficient than the natural fibre reinforced concrete. The load bearing capacity, anchorage and the ductility of the concrete improved with the addition of fibres. According to the experimental findings, artificial fibre reinforced concrete can be employed to increase the structure's strength and longevity as well as to postpone the propagation of cracks. A microstructural analysis of concrete was conducted to ascertain its morphological characteristics.

Keywords: natural fibres; durability; energy absorption; fibre content; crack arrestor; microstructural analysis

Citation: More, F.M.D.S.; Subramanian, S.S. Impact of Fibres on the Mechanical and Durable Behaviour of Fibre-Reinforced Concrete. *Buildings* **2022**, *12*, 1436. https://doi.org/10.3390/buildings12091436

Academic Editor: Ahmed Senouci

Received: 17 August 2022
Accepted: 9 September 2022
Published: 13 September 2022

1. Introduction

Different additives and replacements have been undertaken on conventional concrete to enrich its properties. Much research is under progress on the development of enhanced properties of conventional concrete. One such invention in the concrete is fibre reinforced concrete (FRC). Variant sorts of natural and manufactured fibres have been used to develop FRC. Natural fibres are also developed and added to fibre reinforced concrete in an attempt to protect the environment and promote sustainable development. Coir, jute, sisal, and palm kernel are some of the examples of natural fibres used in fibre reinforced concrete. Owing to its high mechanical characteristics, higher toughness, high impact resistance, and improved energy absorption, fibre reinforced concrete is widely used and researched.

Various factors influence the behaviour of FRC like type of fibre, geometry and orientation of fibres, the aspect ratio of fibres, the distribution of fibres and fibre content.

Ultra-High-Performance Concrete's tensile behavior was improved by the addition of steel and basalt fibres to the concrete (UHPC) [1]. A faster hydration process is observed when mineral fibres and nano silica are added to the concrete [2]. Moreover, the pre-crack energy absorption of the concrete was also low with the higher toughness indices [3]. A scalar damage parameter was used to detect the crack progression effectively in the UPHC model of beam [4]. The matrix strength, shape of the fibre, and the volume fraction of the fibres are responsible for the change in the dynamic increase factor and the transition strain rate of Steel fibre reinforced concrete [5–7]. FA is a useful technique for fine-tuning the hyper-parameters of an RF model. With the help of the Firefly method, the correlation coefficient may be computed over a large number of generations, and the hyperparameters of the Random Forest model for steel fibre reinforced concrete can be tuned [7]. The mechanical properties of concrete get improved with the addition of hooked end steel fibres to the concrete matrix [8]. Glass fibre reinforced concrete is affected by gauge length, geometry, loading type and non-uniform strain distribution [9]. On glass fibre reinforced concrete, a long-term weathering test was undertaken. After analysis, it was determined that as concrete aged and became more alkali resistant, both its tensile strength and ductility decreased [10].

High performance fibre reinforced light weight concrete (HPFRLWC) was made using the addition of polyvinyl alcohol fibres, which showed improved flexural strength along with high flexural ductility and improved toughness of the concrete [11]. With polyvinyl alcohol fibres added to the concrete in low volume fraction, concrete's mechanical characteristics were improved [12]. With the addition of sisal fibres, toughening was observed in the concrete due to crack bridging [13]. Macro plastic fibres were added to the concrete to improve its mechanical properties of the concrete [14]. Various new innovations like self-consolidating concrete and pervious concrete is gaining importance in the construction industries [15]. Despite a drop in compressive strength, the flexural strength and toughness increased with the inclusion of basalt fibres [16]. The addition of metakaolin to the glass fibre reinforced concrete caused the fibres to get pulled out more than the breaking of the fibres. Moreover, the addition of such chemical admixtures did not improve its mechanical properties [17]. Malleated coupling is the most suitable treatment carried out on the natural fibres to improve its mechanical strength performance [18]. The addition of fibres significantly increased the concrete's split tensile and flexural strength, while a slight change was seen in compressive values [19]. For ultra-high-performance concrete with and without the addition of fibres, a correlation between the experimental findings and the numerical data was carried out [20].

The addition of fibres that were subjected to wet or dry cycles early on in the self-compacting concrete's production increased the material's mechanical characteristics by 10 MPa [21]. Hybrid steel/polypropylene fibres added to the concrete resulted in improved post peak ductility and a better failure pattern in the specimens [22]. With the addition of 0.08% polypropylene fibres to the concrete, the resistance of the material to freeze-thaw was found to be higher [23]. Adding polypropylene fibres, nano silica, and silica fume enhances the concrete's qualities [24]. High strength concrete produced with high-performance synthetic macro polypropylene fibres had an increase in compressive strength of 14%, split tensile strength of 17%, and flexural strength of 8.5% (HPP) [25]. With the inclusion of polypropylene, basalt, and glass fibres, fiber-reinforced cemented tailings backfill was created. The findings demonstrated that the use of these fibres increased the concrete's compactness and decreased the progression of cracks [26]. When polypropylene fibres were added to cement-tailings matrix composites, the load bearing capacity post peak increased [27]. Fibre-reinforced cemented tailings backfill possess a dense microstructure with an enhanced interface between the fibre and the cemented tailings backfill matrix (CTB) [28]. Concrete's permeability, flexural toughness, and resistance to chloride attack were all enhanced when high performance polypropylene fibres were added to the mix [29].

Concrete's compressive strength, split tensile strength, and flexural strength were all increased with the addition of fibres and nanoparticles [30].

When high-performance polypropylene fibres were introduced to lightweight concrete, the post-cracking behaviour improved [31]. By adding hybrid steel and polyester fibres to the concrete, plastic shrinkage was minimised by almost 99% [32]. High performance polypropylene fibres enhance the concrete's long-term durability characteristics [33]. The drying shrinkage strain was reduced with the addition of hybrid polypropylene fibres to the concrete. Also, the initial crack formation was delayed with the addition of this fibre [34]. The compressive strength of the mortar was increased by the addition of carbon fibres to the mortar matrix [35]. The compressive strength of the mortar as well as the mortar matrix's capacity for self-sensing were both enhanced by the inclusion of hybrid carbon and brass fibres [36]. By incorporating high-performance polypropylene fibres into the concrete, durability characteristics such chloride penetration, water penetration, sorptivity, and ultrasonic wave velocity are improved [37]. Concrete that has steel and polypropylene fibres added to it has a stronger ability to tolerate deformation than concrete that only has glass fibres because of the latter's brittleness. Additionally, it was noted that the insertion of these fibres increased the load carrying ability [38]. The use of hybrid steel and polypropylene fibres improved the pre-peak and post peak portions of load deflection curves. Non-metallic fibres are added, which helps to seal the microscopic cracks in the concrete and reduces the number of cracks overall [39]. The addition of 2% glass fibres to the lime-based mortar improves the toughness of the mortar and hence enhances the mechanical behaviour [40]. Magnesium phosphate cement (MPC) mortar was supplemented with glass fibres using dosages of 1.5%, 2.5%, and 3.5%. The ideal values were found at 2.5%, and flexural strength increased dramatically [41]. In order to reinforce autoclaved aerated concrete, polypropylene, carbon, basalt, and glass fibres were used. These fibres were added, and the results indicated enhanced compressive and flexural strength. Amongst all of these fibres, carbon fibre reinforced autoclaved aerated concrete showed better results [42].

The concrete's compressive strength and split tensile strength were both improved by 9 to 13% and 20 to 50%, respectively, by the inclusion of glass and polypropylene fibres. [43]. The researchers studied the effects of adding glass, carbon, polyvinyl alcohol, polypropylene, and other fibres to cement mortar that was exposed to high temperatures. Fibres were added in different dosages of 0%, 0.5%, 1%, 1.5% and 2% [44]. Glass and basalt fibres were added to the concrete, which boosted its split tensile strength and flexural strength but had little effect on its compressive strength or elastic modulus values [45]. In a study comparing the mechanical and durability features of glass and polypropylene fibre reinforced concrete, it was found that polypropylene outperformed glass fibre [46]. Furthermore, a temperature study was carried out for glass and polypropylene fibre reinforced concrete to observe the spalling, loss of mass, elastic modulus, and toughness behaviour [47]. Researchers have studied the addition of jute fibres to cementitious composites and it was found that the addition of small amounts of short jute fibres improved the strength of cementitious composites [48]. Steel fibres used in the concrete decreased the slump value while increasing the compressive strength by 17% to 20% [49]. Red pine needle fibres were also added to the concrete in previous studies. The concrete's compressive strength and flexural strength were both enhanced by the application of red pine needle fibres in 40 mm and 30 mm sizes. Additionally, it boosted the concrete's ductility [50]. Concrete's compressive strength and flexural strength were enhanced by using hybrid fibres made of steel and polypropylene [51]. For the concrete, hybrid basalt and steel fibres are used to enhance compressive behaviour. In this hybrid fibre, 0.45% basalt fibres and 0.35% steel fibre were incorporated [52]. Steel fibres with different aspect ratios from 60 to 80 with a volume fraction of 0.35%, 0.45% and 0.55% were studied. The results indicate that the fibres with a higher aspect ratio provided higher compressive strength results [53]. Waste tire steel fibres incorporated into deep beams with openings improved shear capacity and compressive stiffness [54]. Studies on engineering cemented composite concrete beams with carbon

fibre sheets improved the load bearing capacity of the beam [55]. Similarly, the addition of 1.5% steel fibres by volumetric ratio with 600 kg/m^3 as maximum volume of fine aggregate was used to create ultra-high performance fibre reinforced concrete [56]. The effective dispersion of fibres with proper length and aspect ratio determines the development of micro cracks in the concrete [57].

Oil sand from the oil industry can be recycled and used in the building sector in a variety of ways. The fine powder made from oil sand can be incorporated into cement or utilized as a replacement for cementitious material to create new cement-based products. Similarly, the fine and coarse particles of oil sand can be utilized to replace the fine and coarse aggregates used in the construction sector [58]. Roller compacted green concrete is made by substituting oil shale ash for cement [59]. The mechanical properties of roller compacted green concrete were all decreased as compared to roller compacted concrete. This concrete is strong enough to be used for dams and highways [60]. The concrete had the highest strength when Portland cement was replaced with 10% wheat straw ash. Additionally, using 20% wheat straw ash in replacement of Portland cement decreased the permeability and mechanical characteristics of concrete due to the decrease in the water content of the concrete matrix [61–63]. In addition, porosity and durability were also enhanced [64]. In comparison to microbiological concrete, the glass fibre reinforced concrete was stronger. Glass fibre reinforced concrete has a strength improvement of 11.44% [65]. In terms of strength, ductility, and energy absorption capacities, the insertion of double-helix BFRP fibres improves the strain rate sensitivity of concrete, and the rate sensitivity becomes more prominent with an increase in strain rate [66]. By incorporating modified rice straw fibres with grafted Nano-SiO_2 into concrete, the durability performance of RSFRC can be enhanced even more [67]. Due to the fibre bridging effect, the addition of fibres to concrete significantly improves the ductility of concrete. Furthermore, the concrete's reaction to hydration is severely inhibited by the negative curing temperatures [68]. Compared to single fibre reinforced concrete, Basalt and Forta hybrid-fiber reinforced concrete had higher initial strength and energy absorption [69]. The structural performance benefits from the slight weight increase caused by the retrofitting system since the application of an axial load can decrease the lateral displacement of the column under blast load [70].

This research focuses on the FRC experimental examination. Natural and manufactured fibres were employed in this study. The optimization of various FRC was done with compression values. With the optimized fibre content, the other properties were studied. Durability properties, such as water absorption, sorptivity, the volume of permeable voids, acid attack, alkali attack, a rapid chloride permeability test and sulphate attack were investigated. Tests on mechanical properties of FRC were executed after 28 days of water curing. Tests on the durability properties of FRC were executed after 56 days of water curing.

2. Materials and Methods

The maximization of various FRC with distinct fibres were carried out with the determination of compressive results. The concrete grade adopted in this experimental work was M40. Volume fractions of the fibres added were 0%, 0.5%, 1.0%, 1.5%, 2.0% and 2.5%. Optimization was performed with the compression values. Similarly, incorporating the optimum dosage of fibres, the durability study was carried out for 56 days.

2.1. Materials

In this experiment, steel fibres with hooked ends measuring 50 mm in length and 0.60 mm in diameter were used. The fibres implemented in this study are shown in Figure 1. Glass fibres used were 6 mm in length and 22 µm in diameter with an aspect ratio of 273. Carbon fibres used were 5 mm in length and 10 µm in diameter with an aspect ratio of 500. Coir fibres used were 40 mm in length and 0.40 mm in diameter with an aspect ratio of 100. Jute fibres used were 4 mm in length and 20 µm in diameter with an aspect ratio of 200. Sisal fibres used were 40 mm in length and 0.35 mm in diameter with an aspect ratio of 114. The properties of the fibres are presented in Table 1.

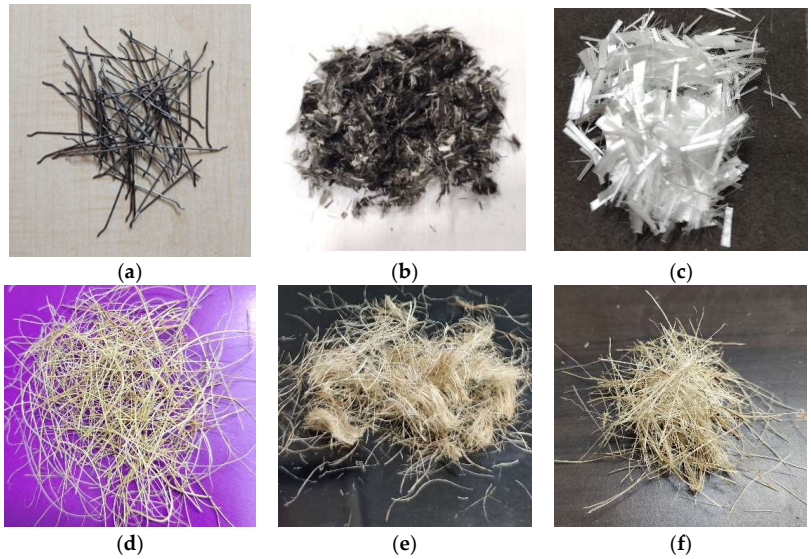

Figure 1. Chopped fibres (**a**) Steel fibre, (**b**) Carbon fibre, (**c**) Glass fibre, (**d**) Coir fibre, (**e**) Jute fibre, (**f**) Sisal fibre.

Table 1. Properties of raw fibres.

Property	Type of Fibre					
	Steel	**Carbon**	**Glass**	**Coir**	**Jute**	**Sisal**
Length	50 mm	5 mm	6 mm	40 mm	4 mm	40 mm
Diameter	0.6 mm	10 µm	22 µm	0.4 mm	20 µm	0.35 mm
Specific gravity	7.8	1.8	2.68	1.5	1.5	1.45
Tensile strength	1800 MPa	4900 MPa	1700 MPa	500 MPa	600 MPa	800 MPa
Water absorption	-	-	-	130–180%	20–40%	75–80%

OPC 53 grade cement with 3.18 specific gravity was adopted in this experimental investigation, conforming to IS12269-2013. River sand, which was available locally, was chosen in this experimental program. The maximum size of fine aggregate was 4.75 mm, satisfying to zone II with reference to Indian Standard 2386–1963. Adopted river sand had a specific gravity of 2.56. Graded crumbled stone of 20 mm and 12.5 mm size was adopted as coarse aggregate confirming to Indian Standard 2386–1963. The crushed stone aggregate adopted was with the specific gravity of 2.69. To enrich the workability of concrete, to minimize the water content and to improve the strength of the concrete, a superplasticizer was used.

In this experimental work, M40 grade concrete was adopted. The mix proportions for M40 grade were taken as 1:2.41:3.77:0.45 with a cement content of 328.33 kg/m^3. The mix calculations are detailed in Table 2.

Table 2. Mix specifications for M40 grade of concrete.

Material	Quantity (kg/m^3)
Cement	328.33
Fine aggregate	791.27
Coarse aggregate	1237.80
Water	147.74
Superplasticizer	4.92

2.2. Experimental Method

In this experimental program, various fibres like steel, carbon, glass, coir, jute and sisal were added with a volumetric ratio of 0%, 0.5%, 1.0%, 1.5%, 2.0% and 2.5%. The

specimens were cured in water for 28 days at room temperature. The optimization of FRC was carried out through compressive strength values. With the optimized dosage the mechanical, durable and microstructural study was carried out.

2.2.1. Determination of Compressive Strength

With reference to IS 516:2018, to evaluate the concrete's compression characteristics, cubical specimens 150 × 150 × 150 mm in size were cast. The cubical specimens were prepared for M40 concrete grade with the addition of variant sorts of fibres, particularly steel, carbon, glass, jute, sisal, and coir. Different fibre fractions were considered, such as 0%, 0.5%, 1.0%, 1.5%, 2.0% and 2.5% by volume of concrete. The specimens were cured in water for 28 days at room temperature. Following the curing stage, the specimens underwent CTM testing at a rate of loading of 4.5 kN/s. Peak compressive strength values were determined for FRC, and the ideal fraction of fibre was determined. The image is represented in Figure 2.

Figure 2. Typical setup of UTM for compressive test.

2.2.2. Determination of Split Tensile Strength

With reference to IS 516:2018, cylinders that were 300 mm tall and 150 mm in diameter were cast. The inclusion of various types of optimal fibres was used to create the cylinders. The specimens were prepared and cured for 28 days. The specimens were cured in water for 28 days at room temperature. Following the curing stage, the specimens underwent CTM testing with a loading rate of 2.5 kN/s The image is represented in Figure 3.

Figure 3. Typical setup of CTM for split tensile test.

2.2.3. Determination of Flexural Strength

With reference to IS 516:2018, beams with dimensions of 100 × 100 × 500 mm were developed. With the inclusion of several types of optimal fibres, prismatic specimens were produced. The specimens were cured in water for 28 days at room temperature. Following the curing stage, the specimens underwent CTM testing with two-point loading condition at

a loading rate of 2.5 kN/s. The supports were positioned 50 mm from either end. The gap between the loadings and the support was set at a fixed distance of 133.33 mm. The image is represented in Figure 4. The flexural strength (f_{cr}) was calculated with the following formula,

$$f_{cr} = \frac{Pl}{bd^2}$$

where,

b = Width of specimen (mm), d = Depth of specimen (mm), l = Length of specimen (mm), P = Ultimate load (N).

Figure 4. Typical setup of CTM for flexure test.

2.2.4. Water Absorption and Porosity

An oven drying method as per ASTM C 642-97 was used. Cylindrical specimens were cut from core of cylinders with the dimensions of 100 mm diameter and 200 mm height. The size of the test specimens used in this test were 100 mm in diameter and 100 mm in height. After curing, the specimens were surface dried and were subjected to water for a minimum of 48 h. Initially, the specimens were kept in an oven with a temperature of 100 °C to 110 °C for 24 h. The temperature of specimens were reduced to room temperature for 24 h and weighed which was taken as A The weights were periodically measured. The specimens were then subjected to water for 48 h and were taken out and surface dried before weighing, and the weight was taken as B. They were then placed in boiling water for a duration of 5 h and cooled to room temperature for 14 h. The weight was then noted and taken as C. Finally, the specimens were hanged with a copper wire and dipped in water with a spring gauge. The weight was noted and taken as D.

2.2.5. Sorptivity

In this work, cylindrical specimens measuring 100 mm in diameter and 50 mm in height were extracted from cylinders of 100 mm in diameter and 200 mm in height as per ASTM C 1585. The specimens were sealed in a container for three days after curing. The specimens were then taken out and sealed along the circumference with an insulation tape. The mass of the specimen at time 0 was taken initially. With a height of 5–10 mm, the cylinders were kept in water. The weight of the specimens was periodically recorded for 1, 2, 3, 4, 9, 12, 16, 20, 25, 30, 45, 60 min, respectively. With the recorded values, the water absorption per unit area can be related by Equation (1),

$$i = S\, t^{0.5} \quad (1)$$

where, S is the sorptivity coefficient, t is the time of weighing, and i is the total amount of water absorbed per unit area.

2.2.6. Rapid Chloride Permeability Test (RCPT)

In this work, cylindrical specimens measuring 100 mm in diameter and 50 mm in height were extracted from cylinders of 100 mm in diameter and 200 mm in height as per ASTM C 1202. The cylinders were projected to 60 V DC supply. The supply was provided for a time period of 6 h, as shown in Figure 5. The RCPT setup was 3% NaCl in one compartment. The other compartment was 3% NaOH.

Figure 5. Typical setup of RCPT.

2.2.7. Acid Attack and Alkali Attack

To investigate the acid impact on concrete, 100 mm-sized cubes were prepared. The cubical specimens were cast and after 24 h they were demoulded. The specimen was maintained in the atmospheric temperature for two days after seven days of water curing. The cubes were then weighed. Then, for 60 days, the cubes were submerged in sulphuric acid. The cubes were maintained in the atmosphere for two days before being weighed. Cubes of 100 mm size were prepared to determine the acid attack of concrete. The cubical specimens were cast and demoulded after 24 h. After seven days the specimen was kept in atmosphere for two days. The cubes were then weighed. These cubes were then immersed in sulphuric acid for 60 days. The cubes were kept in an atmospheric condition for two days and then weighed.

Cubes of 100 mm size were prepared in order to find out the alkali attack of concrete. The cubical specimens were cast and were demoulded after 24 h. After seven days the specimen was kept in atmosphere for two days. The cubes were then weighed. They were then immersed in Na_2SO_4 solution for 60 days. The cubes were kept in an atmospheric condition for two days and then weighed.

2.2.8. Sulphate Attack

Cubes of 150 mm size were prepared to find out the sulphate attack of concrete. The cubes were prepared and demoulded after 24 h. The cubes were then weighed. These cubical specimens were then placed in magnesium sulphate solution for 30 days. After 30 days, the specimens were removed, wiped and tested in a compression testing machine.

3. Results and Discussion

3.1. Compressive Strength

The optimized fraction of fibre addition is determined from the compressive strength values. The addition of fibres reduced the workability and slump of the concrete. The required workability was achieved for all the mixes with the application of superplasticizers to the mix. The graphical illustration of compressive strength values of varietal FRC is presented in Figure 6. The ideal SFRC fraction was found to be 1.5%, with ordinary concrete's compressive strength increasing by 13.69%. With a 3.24% improvement in compressive strength over ordinary concrete, the optimal carbon fraction was found to be 1.5%. The compressive strength value increased with the increase in addition of fibres up to 1.5% volume fraction for steel, carbon, jute and sisal fibres added to the concrete. Also, the compressive strength of glass fibre reinforced concrete increased up to 1% volume fraction.

With a 13.69% improvement in compressive strength over ordinary concrete, the optimal percentage of glass was found to be 1.0%. Similarly, the compressive strength increased up to 2% volume fraction in the case of coir fibre addition. With a 15.92 % improvement in compressive strength over ordinary concrete, the optimal Coir fraction was found to be 2.0%. With a 13.68% gain in compressive strength over ordinary concrete, the optimal jute fraction was found to be 1.5%. Similarly, 1.5% was chosen as the optimal Sisal fraction, and compressive strength was increased by 14.18%.

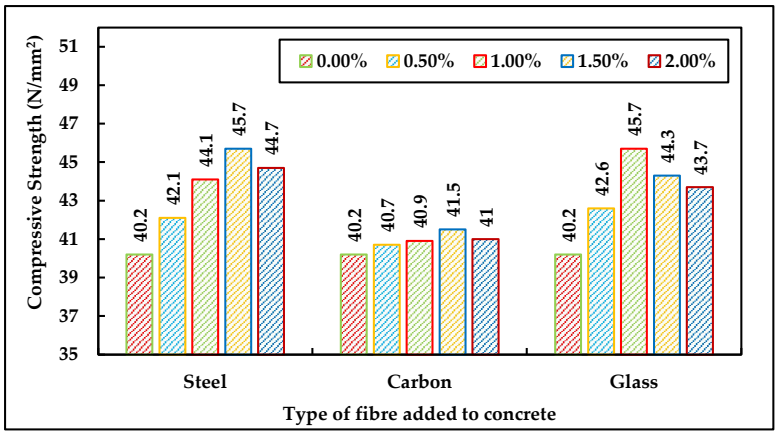

(**a**)

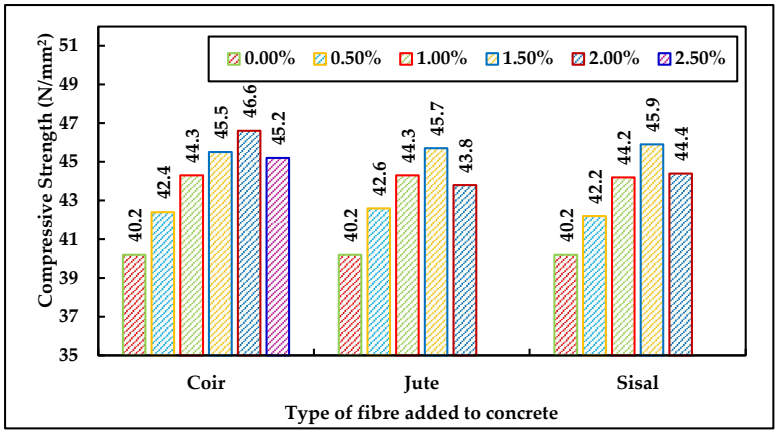

(**b**)

Figure 6. Graphical illustration of compressive strength of FRC. (**a**) Artificial fibre reinforced concrete, (**b**) Natural fibre reinforced concrete.

The reduction of compressive strength after a certain dosage is due to the improper and uneven distribution of fibres within the concrete, leading to the poor homogeneity of the concrete matrix. Based on the results, the compressive strength was affected by volume fraction and the type of fibre added to the concrete. In the case of artificial fibres, the compressive strength was affected by the improper distribution of fibres, whereas in concrete with naturally added fibres, the strength was affected by the balling effect of the fibres with high volume fraction added to the concrete. All the fibre reinforced concrete mixes showed improved compressive strength compared to the control mix. When natural fibres are added to the concrete, the workability is highly affected due to the natural water absorbing ability of the fibres.

3.2. Split Tensile Strength

The results show that the addition of steel fibres increases the split tensile strength maximum when compared to other fibres. This is due to the anchorage provided by the hooked ends of the steel fibre in the concrete matrix. Similarly, the use of certain natural fibres also improves the split tensile strength due to the increased bonding between the

fibres and the concrete matrix. Figure 7 shows a graphical view of split tensile strength data for concrete with varietal fibre reinforcement. Comparing FRC to normal concrete, the percentage gain was 10.37%, 6.99%, 8.11%, 9.46%, 7.66% and 9.01% when reinforced with 1.5% steel, 1.5% carbon, 1.0% glass, 2.0% coir, 1.5% jute and 1.5% sisal fibres by volumetric ratio, respectively. It was also observed that long fibres enhance the split tensile strength compared to the short fibres.

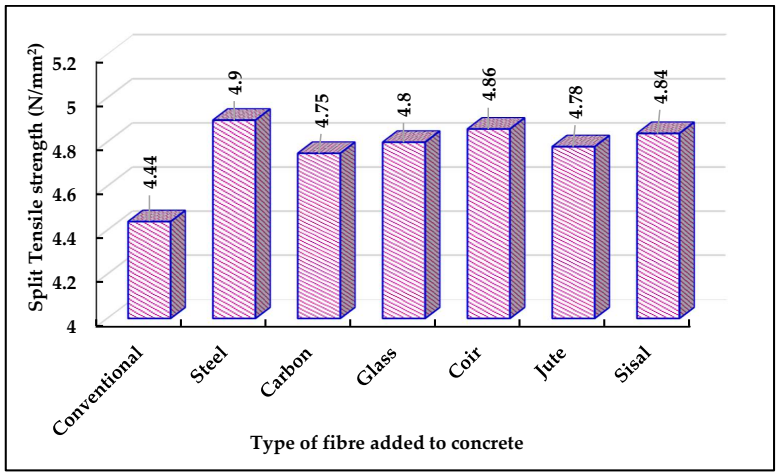

Figure 7. Graphical illustration of split tensile strength of FRC.

3.3. Flexural Strength

The addition of fibres to the concrete improved the flexural strength of the concrete. The addition of fibres makes the concrete matrix more ductile, whereas plain concrete possesses brittle behaviour. The fibres prevent the sudden failure of the member and improves its energy absorption and post cracking behaviour. The uniform distribution of fibres is the main reason for improved flexural strength values. Figure 8 shows a graphical view of flexural strength data for concrete with varietal fibre reinforcement. Comparing FRC to normal concrete, the percentage gain was 12.72%, 16.38%, 12.07%, 15.52%, 12.07% and 13.8% when reinforced with 1.5% steel, 1.5% carbon, 1.0% glass, 2.0% coir, 1.5% jute and 1.5% sisal fibres by volumetric ratio, respectively.

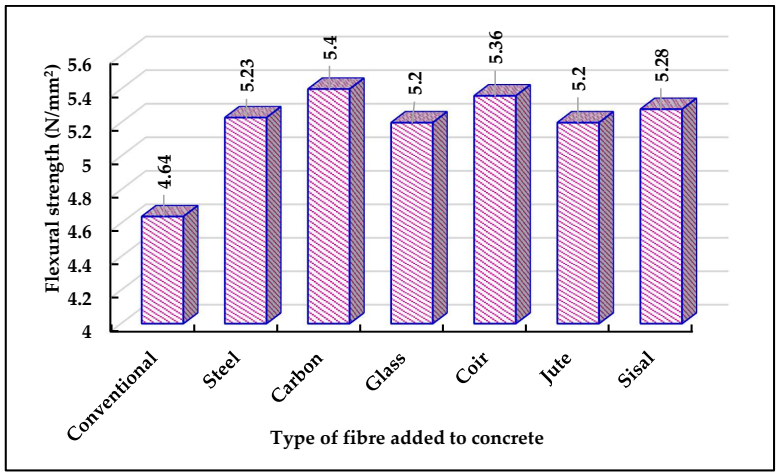

Figure 8. Graphical illustration of flexural strength of FRC.

3.4. Water Absorption and Volume of Permeable Voids

Generally, water absorption of natural fibres is high when compared to artificial fibres. Hence the water absorption of natural fibre reinforced concrete is higher than artificial fibre reinforced concrete. After 56 days of curing, the water absorbed in plain concrete

was derived as 2.09%. With the implementation of 1.5% steel, 1.5% carbon and 1.0% glass fibres, the water absorption was observed as 1.62%, 2.0% and 1.61%, respectively. With the implementation of 2.0% coir, 1.5% jute and 1.5% sisal fibres, the water absorption was observed as 2.79%, 2.84%, and 2.8%, respectively. The graphical illustration is depicted in Figure 9.

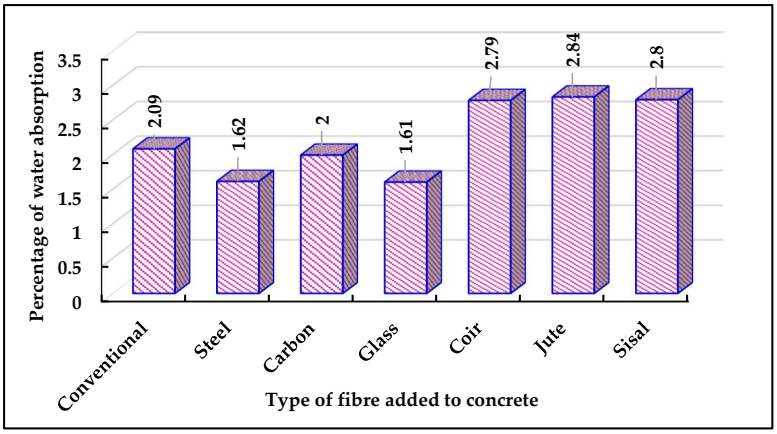

Figure 9. Graphical illustration of water absorption of FRC.

The absorbed water and moisture present in the concrete reacts with the natural fibres and results in the degradation of the fibres, which leads to the formation of voids and pores in the concrete matrix. These voids and pores indirectly affect the strength of the concrete. To effectively use natural fibres considering these properties, suitable coatings can be provided. The porosity of normal concrete was derived as 5.75%, whereas with the implementation of 1.5% steel, 1.5% carbon and 1.0% glass fibres, the porosity was depicted as 4.3%, 4.38% and 4.27%. Due to the incorporation of 2.0% coir, 1.5% jute and 1.5% sisal fibres, the porosity was depicted as 4.65%, 4.86% and 4.53%, respectively. The graphical illustration is depicted in Figure 10.

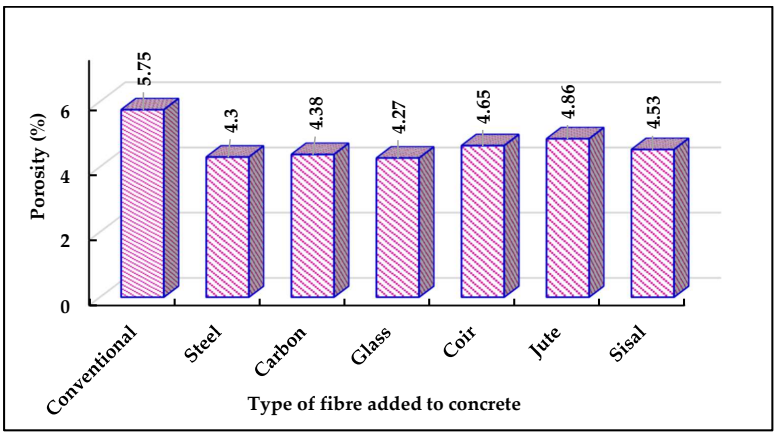

Figure 10. Graphical illustration of porosity of FRC.

3.5. Sorptivity

Sorptivity is the absorption of water into the concrete sample through capillary suction. With a curing duration of 56 days, the sorptivity was determined as 0.002 mm/$t^{0.5}$ for conventional concrete. Similarly, with the incorporation of 1.5% steel, 1.5% carbon, 1.0% glass, 2.0% coir, 1.5% jute and 1.5% sisal fibres, the sorptivity was found as 0.002 mm/$t^{0.5}$, 0.002 mm/$t^{0.5}$, 0.003 mm/$t^{0.5}$, 0.004 mm/$t^{0.5}$, 0.004 mm/$t^{0.5}$ and 0.004 mm/$t^{0.5}$, respectively. The graphical illustration is depicted in Figure 11. Since the water absorption capacity of natural fibres is high, the sorptivity of natural fibres reinforced concrete is slightly higher than the artificial fibre reinforced concrete.

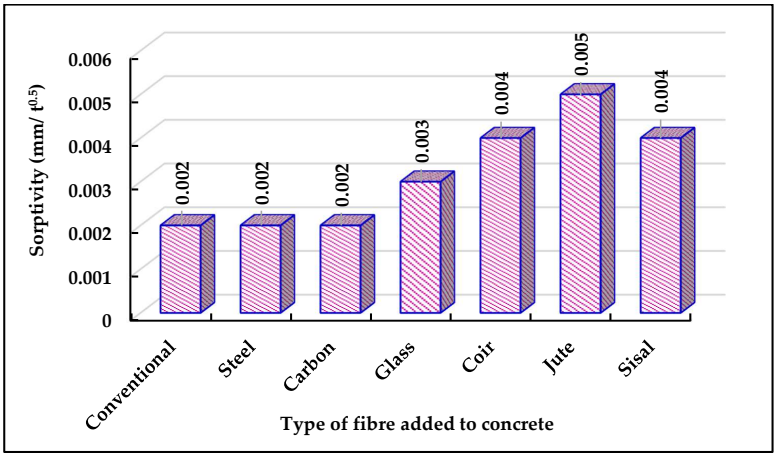

Figure 11. Graphical illustration of sorptivity of FRC.

3.6. Rapid Chloride Permeability Test

Chloride penetration in concrete decreases when artificial fibres are added to the concrete mix. This occurs due to the reduction of pores in the concrete by the addition of artificial fibres. These fibres increase the bonding and compactness between the concrete matrix, thereby reducing the pores in them. Also, these fibres improve the C-S-H in the concrete matrix and hence make it behave better in chloride ion penetration. In contrast, the addition of natural fibres increases the chloride ion penetration in the concrete. This occurs due to the additional pores and voids created in the concrete due to the degradation of natural fibres. The degradation of natural fibres occurs by reacting with the penetrated chloride ion along with the water and moisture present in the concrete matrix. Completing a curing duration of 56 days, the charge passed in the cylindrical specimen of RCPT setup was observed as 1531 coulombs for conventional concrete. Similarly, with the implementation of 1.5% steel, 1.5% carbon, 1.0% glass, 2.0% coir, 1.5% jute and 1.5% sisal fibres, the charge passed was found as 1512 coulombs, 1520 coulombs, 1525 coulombs, 1545 coulombs, 1542 coulombs and 1555 coulombs, respectively. The graphical illustration is depicted in Figure 12.

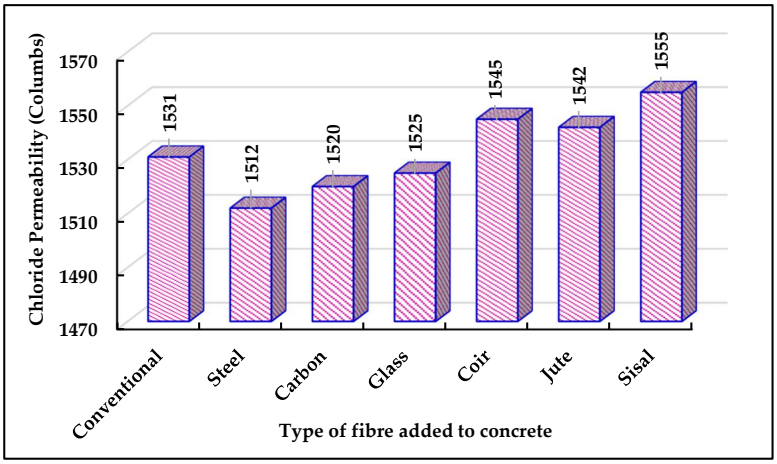

Figure 12. Graphical illustration of Chloride Permeability of FRC.

3.7. Acid Attack and Alkali Attack

Specimens subjected to an acidic environment resulted in internal damage due to the reaction between the acid and the cement matrix. When compared to artificial fibres, natural fibre reinforced concrete has a higher percentage of weight loss. This is due to the formation of voids due to the decomposition of natural fibres in the acidic environment. The chemical reaction between calcium hydroxide or other cement constituents present

in cement paste with the sulphuric acid produces calcium sulphate hydrate (as shown in Equations (2) and (3)), which forms cracks and voids within the concrete and on its surface. The acid attack and impact on the FRC was determined at 70 days curing duration. The weight reduction in conventional concrete was found as 3.31%. With the implementation of 1.5% steel, 1.5% carbon, 1.0% glass fibres, the weight reduction was determined as 3.2%, 3.17% and 3.18% respectively. With the implementation of 2.0% coir, 1.5% jute and 1.5% sisal fibres, the weight reduction was determined as 3.93%, 3.97% and 3.93% respectively. The graphical illustration is depicted in Figure 13.

$$Ca(OH)_2 + H_2SO_4 \longrightarrow CaSO_4.2H_2O \quad (2)$$

$$3CaO.2SiO_2.3H_2O + H_2SO_4 \longrightarrow Ca_2SO_4.2H_2O + Si(OH)_2 \quad (3)$$

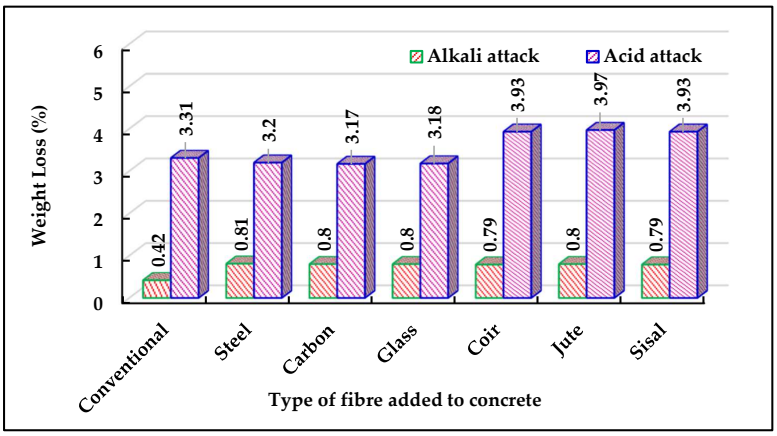

Figure 13. Graphical illustration of weight loss of FRC due to acid attack and alkali attack.

The calcium hydroxide from the cement paste reacts with sodium sulphate to form calcium sulphate hydrate (as shown in Equation (4)), which reacts with calcium silicate hydrate C-S-H in concrete matrix making the bonding weak. Hence, the strength reduces. Since the sodium sulphate does not easily penetrate the concrete, the formation of calcium sulphate hydrate is lower than acid attack. The attack and impact on the FRC due to alkali was determined at 70 days curing duration. The weight loss in conventional concrete was found as 0.42%. With the implementation of 1.5% steel, 1.5% carbon, and 1.0% glass fibres, the weight loss was determined as 0.81%, 0.8% and 0.8%, respectively. With the implementation of 2.0% coir, 1.5% jute and 1.5% sisal fibres, the weight loss was determined as 0.79%, 0.8% and 0.79%, respectively. The graphical illustration is depicted in Figure 13.

$$Na_2SO_4 + Ca(OH)_2 + 2H_2O \longrightarrow Ca_2SO_4.2H_2O + 2NaOH \quad (4)$$

3.8. Sulphate Attack

Specimens subjected to sulphate environment undergo a chemical reaction within the concrete, creating voids and pores. The chemical reaction breaks the C-S-H in the concrete matrix and hence reduces the bonding and strength of the concrete. The magnesium sulphate reacts with calcium hydroxide in cement paste and water to produce calcium sulphate hydrate (as shown in Equation (5)), causing internal voids and cracks. With the exposure to the sulphate environment, the compressive strength was decreased by 4.23% in conventional concrete. Similarly, with the implementation of 1.5% steel, 1.5% carbon, 1.0% glass, 2.0% coir, 1.5% jute and 1.5% sisal fibres, the values were reduced by 6.13%, 4.1%, 4.82%, 3.87%, 4.38% and 6.11% respectively, as shown in Figure 14.

$$MgSO_4 + Ca(OH)_2 + 2H_2O \longrightarrow Ca_2SO_4.2H_2O + Mg(OH)_2 \quad (5)$$

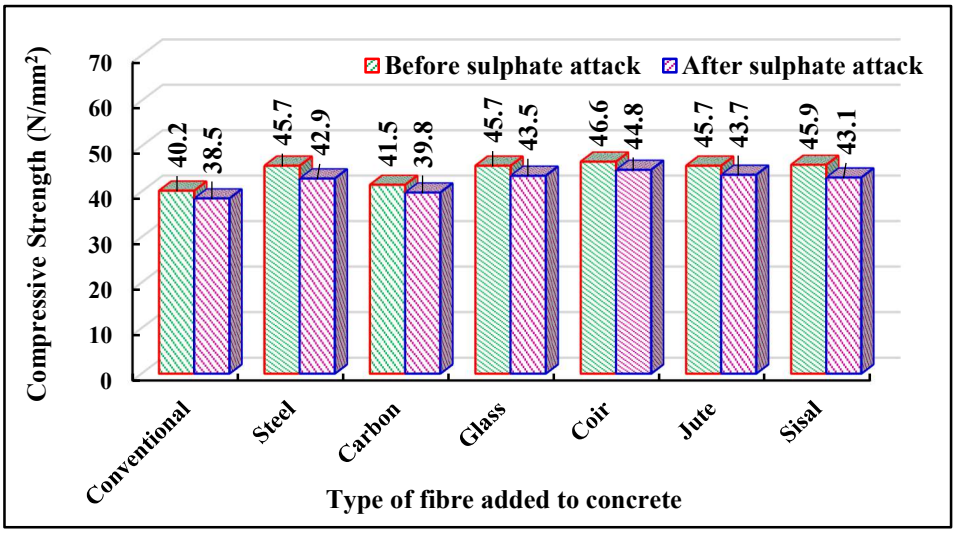

Figure 14. Graphical illustration of compressive strength of FRC due to sulphate attack.

3.9. Micro-Structural Study

Fibre-reinforced concrete and conventional concrete were imaged using a scanning electron microscope (SEM). Adding fibres to the concrete improved the bonding between the different parts of the concrete. The fibre insertion improved anchoring in the concrete matrix and served as a link between the concrete matrix. Figure 15 displays SEM images of both ordinary concrete and fibre reinforced concrete. The strengths of fibre reinforced concrete were more clearly visible than those of ordinary concrete because it offered superior anchoring. Concrete with artificial fibre additions bonded better than concrete with natural fibre additions. Voids were observed in the natural fibre reinforced concrete due to the degradation of fibres with the entrapped moisture in the concrete. A uniform distribution of fibres were observed in the fibre reinforced concrete. When carbon fibres were added to the concrete matrix, the carbon fibres were not effectively dispersed like the other types of fibre reinforced concrete. Therefore, dispersing agents can be used to effectively disperse the fibres and enhance the strength.

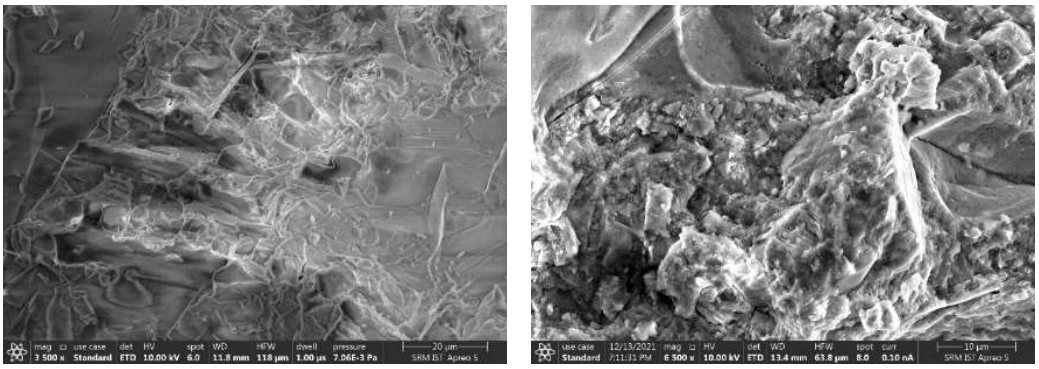

(**a**) (**b**)

Figure 15. *Cont.*

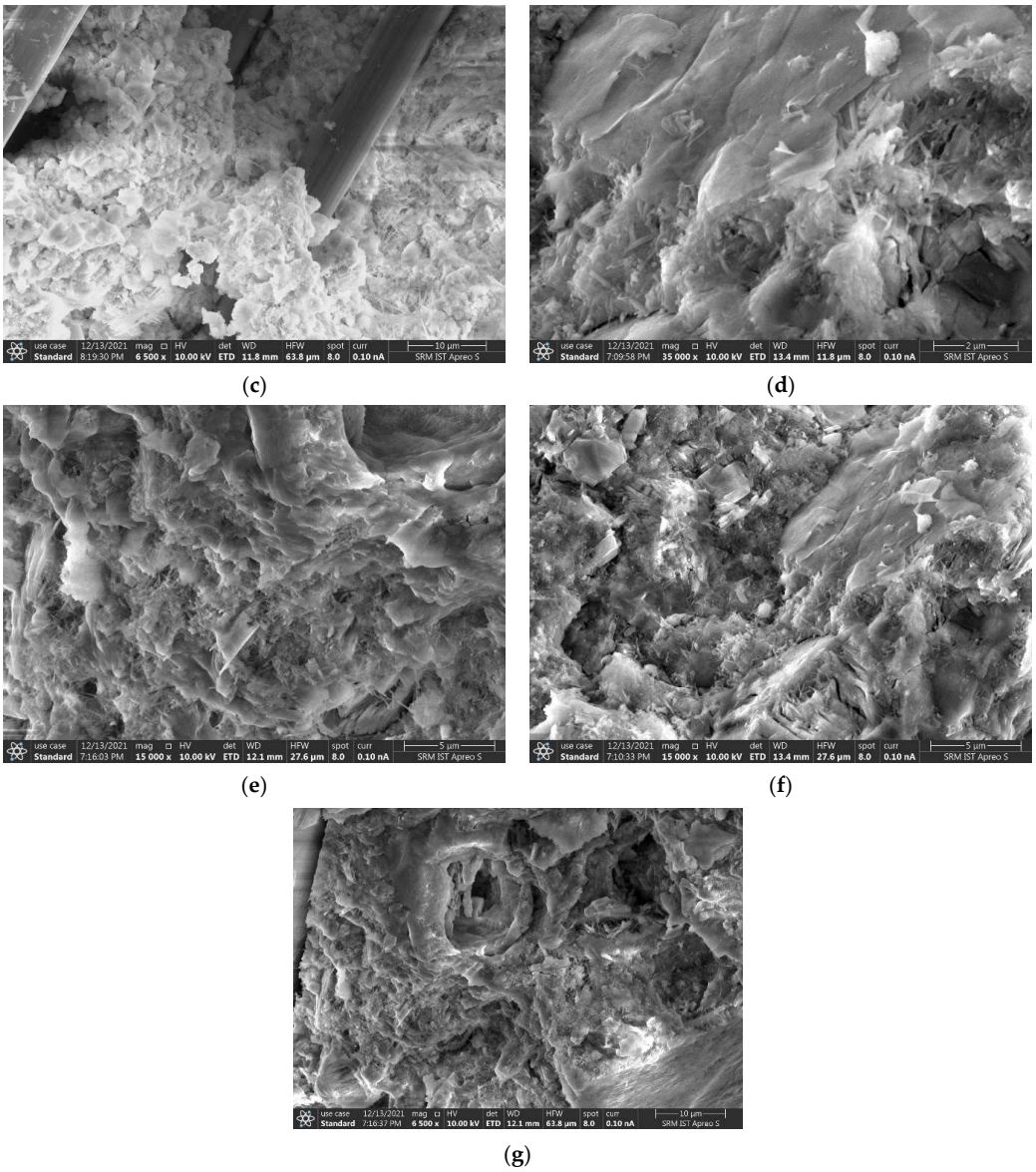

Figure 15. SEM Images: (**a**) Conventional Concrete, (**b**) Steel fibre reinforced concrete, (**c**) Carbon fibre reinforced concrete, (**d**) Glass fibre reinforced concrete, (**e**) Coir fibre reinforced concrete, (**f**) Jute fibre reinforced concrete, (**g**) Sisal fibre reinforced concrete.

To determine the crystalline impact of the concrete, X-ray powder diffraction (XRD) was applied to each sample. In every sample, the hydration components were visible. Contrary to conventional concrete and natural fibre reinforced concrete, higher peaks of dicalcium silicate and tricalcium silicate were found in artificial fibre reinforced concrete, as shown in Figure 16. In FRC samples, quartz production was also detected. All of the concrete samples had tiny peaks of calcium carbonate crystals as well. This is the result of a chemical reaction between the water molecules added to the cement particles during the concrete preparation process and the cement particles themselves. In comparison to conventional concrete samples, fibre reinforced concrete samples were found to have greater portlandite and ettringite peak concentrations.

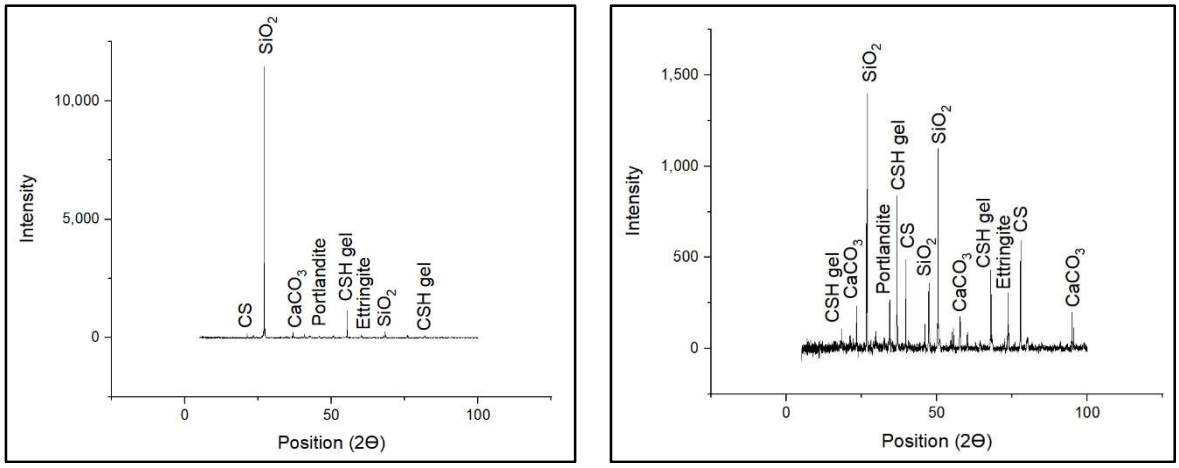

(**a**) (**b**)

Figure 16. XRD results: (**a**) Conventional Concrete, (**b**) fibre reinforced concrete.

4. Conclusions

The mechanical performance of fibre reinforced concrete has undergone much research and development in recent decades. The use of appropriate admixtures, improved fibre selection, and uniform fibre dispersion have all led to improvements in performance. In this study, the research on the strength and durability effects of various fibre reinforced concrete has been reviewed. After the experimental investigation performed on the FRC with varietal distinct fibres was concluded, the following conclusions were reached:

1. The ideal fraction of fibres added was determined to be 1.5% for steel, 1.5% for carbon, 1.0% for glass, 2.0% for coir, 1.5% for jute, and 1.5% for sisal. The compressive strength of the fibre reinforced concrete increased up to the optimum percentage, and reduced thereafter. This occurs due to the poor homogeneity in the concrete caused by the improper distribution of fibres.
2. The split tensile strength of FRC increased notably with the maximum increase in steel fibre reinforced concrete with a value of 10.37%. It was also observed that the split tensile strength was higher for long fibres than for short fibres.
3. The flexural strength of FRC was high when equated with conventional concrete results, with the maximum in carbon fibre reinforced concrete with a value of 16.38%. The addition of fibres increased the ductility of the concrete, improving the post cracking behaviour of the concrete and increasing the strength of the concrete.
4. The absorption of water was found to be a little higher in natural fibre infused concrete than the manufactured fibre added and the plain concrete. This was due to the natural water absorption capacity present in these fibres, which can be overcome by the application of coatings to the fibres.
5. The chloride permeability in FRC with the addition of varietal distinct fibres was low, ranging between 1000–2000 coulombs. The weight loss in concrete was a little higher in natural fibre added concrete when exposed to an acidic environment, whereas the weight loss was minimal for all the mix in an alkaline environment. The behaviour of the concrete in terms of the durability aspect was better when compared to conventional concrete.
6. When compared to normal concrete, artificial fibre reinforced concrete has been shown to have better mechanical and durability properties. Additionally, the use of fibres slows the development and spread of cracks, preventing any member from sudden failure.
7. Similarly, the natural fibre reinforced concrete behaves better in terms of mechanical properties, whereas it is less effective with regard to durability. This is due to the natural water absorption and degradation effect of the fibres.
8. The mechanical properties of the concrete are enhanced by the addition of fibres. On the other hand, artificial fibre reinforced concrete performs better in terms of

durability than natural fibre reinforced concrete. This is due to the lack of surface treatment provided to the natural fibres. Therefore, similar future experiments can be conducted by employing various types of treatments to natural fibres to minimize their capacity to absorb water and degrade.

Therefore, natural fibres can be effectively used as an additive to enrich the properties and to create a sustainable development in environment. Treatments to natural fibres can be implemented to reduce the water absorption of these fibres and to improve its behaviour much more significantly.

Author Contributions: Conceptualization, F.M.D.S.M. and S.S.S.; methodology, F.M.D.S.M.; validation, F.M.D.S.M. and S.S.S.; experimental investigation, F.M.D.S.M.; supervision, S.S.S.; project administration, F.M.D.S.M. and S.S.S. All authors have read and agreed to the published version of the manuscript.

Funding: This research received no external funding.

Data Availability Statement: The data presented in this study are available on request from the corresponding author.

Conflicts of Interest: This manuscript has not been submitted to, nor is it under review by, another journal or other publishing venue. The authors have no affiliation with any organization with a direct or indirect financial interest in the subject matter discussed in the manuscript. The authors declare that they have no conflicts of interest.

References

1. Kang, S.-T.; Choi, J.-I.; Koh, K.-T.; Lee, K.S.; Lee, B.Y. Hybrid effects of steel fiber and microfiber on the tensile behavior of ultra-high performance concrete. *Compos. Struct.* **2016**, *145*, 37–42. [CrossRef]
2. Larisa, U.; Solbon, L.; Sergei, B. Fiber-reinforced Concrete with Mineral Fibers and Nanosilica. *Procedia Eng.* **2017**, *195*, 147–154. [CrossRef]
3. Khan, M.; Ali, M. Use of glass and nylon fibers in concrete for controlling early age micro cracking in bridge decks. *Constr. Build. Mater.* **2016**, *125*, 800–808. [CrossRef]
4. Solhmirzaei, R.; Kodur, V. Modeling the response of ultra high performance fiber reinforced concrete beams. *Procedia Eng.* **2017**, *210*, 211–219. [CrossRef]
5. Yang, L.; Lin, X.; Gravina, R.J. Evaluation of dynamic increase factor models for steel fibre reinforced concrete. *Constr. Build. Mater.* **2018**, *190*, 632–644. [CrossRef]
6. Yang, L.; Lin, X.; Li, H.; Gravina, R.J. A new constitutive model for steel fibre reinforced concrete subjected to dynamic loads. *Compos. Struct.* **2019**, *221*, 110849. [CrossRef]
7. Yang, L.; Qi, C.; Lin, X.; Li, J.; Dong, X. Prediction of dynamic increase factor for steel fibre reinforced concrete using a hybrid artificial intelligence model. *Eng. Struct.* **2019**, *189*, 309–318. [CrossRef]
8. More, D.F.; Selvan, S.S. Experimental study on addition of Steel Fibres in Conventional Concrete. *IOP Conf. Series Mater. Sci. Eng.* **2021**, *1130*, 012044. [CrossRef]
9. Mobasher, B.; Shah, S.P. Test parameters for evaluating toughness of glass-fiber reinforced concrete panels. *ACI Mater. J.* **1989**, *86*, 448–458.
10. Shah, S.P.; Ludirdja, D.; Daniel, J.I.; Mobasher, B. Toughness-durability of glass fiber reinforced concrete systems. *ACI Mater. J.* **1988**, *85*, 352–360.
11. Arisoy, B.; Wu, H.-C. Material characteristics of high performance lightweight concrete reinforced with PVA. *Constr. Build. Mater.* **2008**, *22*, 635–645. [CrossRef]
12. Noushini, A.; Samali, B.; Vessalas, K. Effect of polyvinyl alcohol (PVA) fibre on dynamic and material properties of fibre reinforced concrete. *Constr. Build. Mater.* **2013**, *49*, 374–383. [CrossRef]
13. Savastano, H.; Santos, S.; Radonjic, M.; Soboyejo, W. Fracture and fatigue of natural fiber-reinforced cementitious composites. *Cem. Concr. Compos.* **2009**, *31*, 232–243. [CrossRef]
14. Yin, S.; Tuladhar, R.; Shi, F.; Combe, M.; Collister, T.; Sivakugan, N. Use of macro plastic fibres in concrete: A review. *Constr. Build. Mater.* **2015**, *93*, 180–188. [CrossRef]
15. Mehta, P.K.; Monteiro, P.J.M. *Concrete: Microstructure, Properties and Materials*, 4th ed.; McGraw-Hill Professional: New York, NY, USA, 2014.
16. Sadrmomtazi, B.; Saradar, T.A. Effects of silica fume on mechanical strength and microstructure of basalt fiber reinforced cementitious composites (BFRCC). *Constr. Build. Mater.* **2018**, *162*, 321–333. [CrossRef]
17. Enfedaque, A.; Cendón, D.; Gálvez, F.; Sánchez-Gálvez, V. Analysis of glass fiber reinforced cement (GRC) fracture surfaces. *Constr. Build. Mater.* **2010**, *24*, 1302–1308. [CrossRef]

18. Koohestani, A.K.; Darban, P.; Mokhtari, E.; Darezereshki, Y.E. Comparison of different natural fiber treatments: A literature review. *Int. J. Environ. Sci. Technol.* **2019**, *16*, 629–642. [CrossRef]
19. Wu, T.; Yang, X.; Wei, H.; Liu, X. Mechanical properties and microstructure of lightweight aggregate concrete with and without fibers. *Constr. Build. Mater.* **2018**, *199*, 526–539. [CrossRef]
20. Chi, Y.; Min, Y.; Huang, L.; Xu, L. Finite element modeling of steel polypropylene hybrid fiber reinforced concrete using modified concrete damaged plasticity. *Eng. Struct.* **2017**, *148*, 23–35. [CrossRef]
21. Yehia, S.; Douba, A.; Abdullahi, O.; Farrag, S. Mechanical and durability evaluation of fiber-reinforced self-compacting concrete. *Constr. Build. Mater.* **2016**, *121*, 120–133. [CrossRef]
22. Li, B.; Chi, Y.; Xu, L.; Shi, Y.; Li, C. Experimental investigation on the flexural behavior of steel-polypropylene hybrid fiber reinforced concrete. *Constr. Build. Mater.* **2018**, *191*, 80–94. [CrossRef]
23. Zhang, P.; Li, Q.-F. Effect of polypropylene fiber on durability of concrete composite containing fly ash and silica fume. *Compos. Part B Eng.* **2013**, *45*, 1587–1594. [CrossRef]
24. Fallah, S.; Nematzadeh, M. Mechanical properties and durability of high-strength concrete containing macro-polymeric and polypropylene fibers with nano-silica and silica fume. *Constr. Build. Mater.* **2017**, *132*, 170–187. [CrossRef]
25. Abaeian, R.; Behbahani, H.P.; Moslem, S.J. Effects of high temperatures on mechanical behavior of high strength concrete reinforced with high performance synthetic macro polypropylene (HPP) fibres. *Constr. Build. Mater.* **2018**, *165*, 631–638. [CrossRef]
26. Cao, S.; Yilmaz, E.; Song, W. Fiber type effect on strength, toughness and microstructure of early age cemented tailings backfill. *Constr. Build. Mater.* **2019**, *223*, 44–54. [CrossRef]
27. Xue, G.; Yilmaz, E.; Song, W.; Cao, S. Mechanical, flexural and microstructural properties of cement-tailings matrix composites: Effects of fiber type and dosage. *Compos. Part B Eng.* **2019**, *172*, 131–142. [CrossRef]
28. Xue, G.; Yilmaz, E.; Song, W.; Yilmaz, E. Influence of fiber reinforcement on mechanical behavior and microstructural properties of cemented tailings backfill. *Constr. Build. Mater.* **2019**, *213*, 275–285. [CrossRef]
29. Behfarnia, K.; Behravan, A. Application of high performance polypropylene fibers in concrete lining of water tunnels. *Mater. Des.* **2014**, *55*, 274–279. [CrossRef]
30. Beigi, M.H.; Berenjian, J.; Omran, O.L.; Nik, A.S.; Nikbin, I.M. An experimental survey on combined effects of fibers and nanosilica on the mechanical, rheological, and durability properties of self-compacting concrete. *Mater. Des.* **2013**, *50*, 1019–1029. [CrossRef]
31. Li, J.J.; Niu, J.G.; Wan, C.J.; Jin, B.; Yin, Y.L. Investigation on mechanical properties and microstructure of high performance polypropylene fiber reinforced lightweight aggregate concrete. *Constr. Build. Mater.* **2016**, *118*, 27–35. [CrossRef]
32. Sivakumar, A.; Santhanam, M. A quantitative study on the plastic shrinkage cracking in high strength hybrid fiber reinforced concrete. *Cement. Concr. Compos.* **2007**, *29*, 575–581. [CrossRef]
33. Afroughsabet, V.; Ozbakkaloglu, T. Mechanical and durability properties of high-strength concrete containing steel and polypropylene fibers. *Constr. Build. Mater.* **2015**, *94*, 73–82. [CrossRef]
34. Hsie, M.; Tu, C.; Song, P.S. Mechanical properties of polypropylene hybrid fiber-reinforced concrete. *Mater. Sci. Eng. A* **2008**, *494*, 153–157. [CrossRef]
35. Ram, K.D.; Thirumurugan, V.; Satyanarayanan, K.S. Experimental study on optimization of smart mortar with the addition of brass fibres. *Mater. Today Proc.* **2022**, *50*, 388–393.
36. Durairaj, R.; Varatharajan, T.; Srinivasan, S.K.; Gurupatham, B.G.A.; Roy, K. An Experimental Study on Electrical Properties of Self-Sensing Mortar. *J. Compos. Sci.* **2022**, *6*, 208. [CrossRef]
37. Ramezanianpour, A.; Esmaeili, M.; Ghahari, S.; Najafi, M. Laboratory study on the effect of polypropylene fiber on durability, and physical and mechanical characteristic of concrete for application in sleepers. *Constr. Build. Mater.* **2013**, *44*, 411–418. [CrossRef]
38. Simões, T.; Costa, H.; Dias-Da-Costa, D.; Julio, E. Influence of fibres on the mechanical behaviour of fibre reinforced concrete matrixes. *Constr. Build. Mater.* **2017**, *137*, 548–556. [CrossRef]
39. Sivakumar, A.; Santhanam, M. Mechanical properties of high strength concrete reinforced with metallic and non-metallic fibres. *Cem. Concr. Compos.* **2007**, *29*, 603–608. [CrossRef]
40. Iucolano, F.; Liguori, B.; Colella, C. Fibre-reinforced lime-based mortars: A possible resource for ancient masonry restoration. *Constr. Build. Mater.* **2013**, *38*, 785–789. [CrossRef]
41. Fang, Y.; Chen, B.; Oderji, S.Y. Experimental research on magnesium phosphate cement mortar reinforced by glass fiber. *Constr. Build. Mater.* **2018**, *188*, 729–736. [CrossRef]
42. Pehlivanlı, Z.O.; Uzun, I.; Demir, I. Mechanical and microstructural features of autoclaved aerated concrete reinforced with autoclaved polypropylene, carbon, basalt and glass fiber. *Constr. Build. Mater.* **2015**, *96*, 428–433. [CrossRef]
43. Choi, Y.; Yuan, R.L. Experimental relationship between splitting tensile strength and compressive strength of GFRC and PPFRC. *Cem. Concr. Res.* **2005**, *35*, 1587–1591. [CrossRef]
44. Çavdar, A. A study on the effects of high temperature on mechanical properties of fiber reinforced cementitious composites. *Compos. B Eng.* **2012**, *43*, 2452–2463. [CrossRef]
45. Arslan, M.E. Effects of basalt and glass chopped fibers addition on fracture energy and mechanical properties of ordinary concrete: CMOD measurement. *Constr. Build. Mater.* **2016**, *114*, 383–391. [CrossRef]
46. Liu, J.; Jia, Y.; Wang, J. Experimental Study on Mechanical and Durability Properties of Glass and Polypropylene Fiber Reinforced Concrete. *Fibers Polym.* **2019**, *20*, 1900–1908. [CrossRef]

47. Wu, H.; Lin, X.; Zhou, A. A review of mechanical properties of fibre reinforced concrete at elevated temperatures. *Cem. Concr. Res.* **2020**, *135*, 106117. [CrossRef]
48. Song, H.; Liu, J.; He, K.; Ahmad, W. A comprehensive overview of jute fiber reinforced cementitious composites. *Case Stud. Constr. Mater.* **2021**, *15*, e00724. [CrossRef]
49. Samarakoon, S.S.M.; Ruben, P.; Pedersen, J.W.; Evangelista, L. Mechanical performance of concrete made of steel fibers from tire waste. *Case Stud. Constr. Mater.* **2019**, *11*, e00259. [CrossRef]
50. Cogurcu, M.T. Investigation of mechanical properties of red pine needle fiber reinforced self-compacting ultra high performance concrete. *Case Stud. Constr. Mater.* **2022**, *16*, e00970. [CrossRef]
51. El Ouni, M.H.; Shah, S.H.A.; Ali, A.; Muhammad, S.; Mahmood, M.S.; Ali, B.; Marzouki, R.; Raza, A. Mechanical performance, water and chloride permeability of hybrid steel-polypropylene fiber-reinforced recycled aggregate concrete. *Case Stud. Constr. Mater.* **2022**, *16*, e00831. [CrossRef]
52. Khan, M.; Cao, M.; Xie, C.; Ali, M. Effectiveness of hybrid steel-basalt fiber reinforced concrete under compression. *Case Stud. Constr. Mater.* **2022**, *16*, e00941. [CrossRef]
53. Alrawashdeh, A.; Eren, O. Mechanical and physical characterisation of steel fibre reinforced self-compacting concrete: Different aspect ratios and volume fractions of fibres. *Results Eng.* **2022**, *13*, 100335. [CrossRef]
54. Augustino, D.S.; Kabubo, C.; Kanali, C.; Onchiri, R.O. The orientation effect of opening and internal strengthening on shear performance of deep concrete beam using recycled tyre steel fibres. *Results Eng.* **2022**, *15*, 100561. [CrossRef]
55. Ge, W.; Tang, R.; Wang, Y.; Zhang, Z.; Sun, C.; Yao, S.; Lu, W. Flexural performance of ECC-concrete composite beams strengthened with carbon fiber sheet. *Results Eng.* **2022**, *13*, 100334. [CrossRef]
56. Tamataki, K.; Ito, T.; Fujino, Y.; Yoshitake, I. Development of an Ultra-High-Performance Fibre-Reinforced Concrete (UHPFRC) Manufacturable at Ambient Temperature. *Buildings* **2022**, *12*, 740. [CrossRef]
57. Hrabová, K.; Láník, J.; Lehner, P. Statistical and Practical Evaluation of the Mechanical and Fracture Properties of Steel Fibre Reinforced Concrete. *Buildings* **2022**, *12*, 1082. [CrossRef]
58. Hesham, N.; Moncef, L.N.; Kırgız, M.S. Characteristic properties of the treated by-product of oil shale ash. *J. Adv. Compos. Mater. Constr. Environ. Nano Technol.* **2021**, *4*, 1–11. Available online: http://onlinejournal.org.uk/index.php/JC2MENT/article/view/584 (accessed on 8 September 2022).
59. Ashteyat, A.; Al Rjoub, Y.S.; Smadi, A.; Kırgız, M.S. Reuse of oil shale ash in the roller compacted concrete for earthquake engineering and durability. *J. Adv. Compos. Mater. Constr. Environ. Nano Technol.* **2020**, 1–20. Available online: http://onlinejournal.org.uk/index.php/JC2MENT/article/view/564 (accessed on 8 September 2022).
60. Ashteyat, A.; Kırgız, M.S.; Al Rjoub, Y.S.; Smadi, A.; Obaidat, A.T. Roller Compacted Concrete with Oil Shale Ash as a Replacement of Cement: Mechanical and Durability Behavior. *Int. J. Pavement Res. Technol.* **2022**. Available online: https://www.researchgate.net/publication/362453243_Roller_Compacted_Concrete_with_Oil_Shale_Ash_as_a_Replacement_of_Cement_Mechanical_and_Durability_Behavior (accessed on 8 September 2022).
61. Katman, H.Y.; Wang, J.K.; Bheel, N.D.; Kirgiz, M.S.; Kumar, A.; Khatib, J.; Benjeddou, O. Workability, strength, modulus of elasticity, and permeability feature of wheat straw ash-incorporated hydraulic cement concrete. *Buildings* **2022**, *12*, 1363. Available online: https://www.researchgate.net/publication/362889157_Workability_strength_modulus_of_elasticity_and_permeability_feature_of_wheat_straw_ash-incorporated_hydraulic_cement_concrete (accessed on 8 September 2022). [CrossRef]
62. Bheel, N.; Ali, M.O.A.; Kırgız, M.S.; Galdino, A.G.d.S.; Kumar, A. Fresh and mechanical properties of concrete made of binary substitution of millet husk ash and wheat straw ash for cement and fine aggregate. *J. Mater. Res. Technol.* **2021**, *13*, 872–893. [CrossRef]
63. Biricik, H.; Kırgız, M.S.; Karapınar, I.S. Advances in physical and mechanical properties of wheat straw ash-substituted-cement mortar. *ZKG Int.* **2021**, *3*, 43–55. Available online: https://www.zkg.de/en/artikel/zkg_Advances_in_physical_and_mechanical_properties_of_wheat_straw_ash_3645294.html (accessed on 8 September 2022).
64. Biricik, H.; Kırgız, M.S.; Oluwaseun, P.O.; Erenoğlu, T. Characteristic properties of wheat straw ash and its effects on the physical, mechanical, and durability properties of mortar. *J. Adv. Compos. Mater. Constr. Environ. Nano Technol.* **2020**, *2020*, 47–64. Available online: http://onlinejournal.org.uk/index.php/JC2MENT/article/view/572 (accessed on 8 September 2022).
65. Manojkumar, C.; Ramesh, B.; Kumar, G.R. Study on the compressive strength of glass fibre reinforced M20 grade self-healing concrete using a novel technique microbial induced calcite precipitation. *Mater. Today Proc.* **2022**, in press. [CrossRef]
66. Zhang, C.; Hao, H.; Hao, Y. Experimental study of mechanical properties of double-helix BFRP fiber reinforced concrete at high strain rates. *Cem. Concr. Compos.* **2022**, *132*, 104633. [CrossRef]
67. Liu, J.; Xie, X.; Li, L. Experimental study on mechanical properties and durability of grafted nano-SiO2 modified rice straw fiber reinforced concrete. *Constr. Build. Mater.* **2022**, *347*, 128575. [CrossRef]
68. Lu, J.; Liu, J.; Yang, H.; Gao, J.; Wan, X.; Zhang, J. Influence of curing temperatures on the performances of fiber-reinforced concrete. *Constr. Build. Mater.* **2022**, *339*, 127640. [CrossRef]
69. Taghipoor, H.; Sadeghian, A. Experimental investigation of single and hybrid-fiber reinforced concrete under drop weight test. *Structures* **2022**, *43*, 1073–1083. [CrossRef]
70. Hanifehzadeh, M.; Aryan, H.; Gencturk, B.; Akyniyazov, D. Structural Response of Steel Jacket-UHPC Retrofitted Reinforced Concrete Columns under Blast Loading. *Materials* **2021**, *14*, 1521. [CrossRef]